TECHNICAL NOTE

D-940

LANDING CHARACTERISTICS OF A LENTICULAR-SHAPED

REENTRY VEHICLE

By Ulysse J. Blanchard

Langley Research Center
Langley Field, Va.

NATIONAL AERONAUTICS AND SPACE ADMINISTRATION

WASHINGTON   September 1961

NATIONAL AERONAUTICS AND SPACE ADMINISTRATION

TECHNICAL NOTE D-940

LANDING CHARACTERISTICS OF A LENTICULAR-SHAPED

REENTRY VEHICLE

By Ulysse J. Blanchard

SUMMARY

An experimental investigation was made of the landing characteristics of a 1/9-scale dynamic model of a lenticular-shaped reentry vehicle having extendible tail panels for control after reentry and for landing control (flare-out). The landing tests were made by catapulting a free model onto a hard-surface runway and onto water. A "belly-landing" technique in which the vehicle was caused to skid and rock on its curved undersurface (heat shield), converting sinking speed into angular energy, was investigated on a hard-surface runway. Landings were made in calm water and in waves both with and without auxiliary landing devices. Landing motions and acceleration data were obtained over a range of landing attitudes and initial sinking speeds during hard-surface landings and for several wave conditions during water landings. A few vertical landings (parachute letdown) were made in calm water.

The hard-surface landing characteristics were good. Maximum landing accelerations on a hard surface were 5g and 18 radians per second^2 over a range of landing conditions. Horizontal landings on water resulted in large violent rebounds and some diving in waves. Extreme attitude changes during rebound at initial impact made the attitude of subsequent impact random. Maximum accelerations for water landings were approximately 21g and 145 radians per second^2 in waves 7 feet high. Various auxiliary water-landing devices produced no practical improvement in behavior. Reduction of horizontal speed and positive control of impact attitude did improve performance in calm water. During vertical landings in calm water maximum accelerations of 15g and 110 radians per second^2 were measured for a contact attitude of -45° and a vertical velocity of 70 feet per second.

INTRODUCTION

The requirements for multimanned lunar missions indicate that the reentry vehicle should be of such shape as to minimize the launch vehicle's control and structural loading problems. In addition, reentry guidance accuracies and impact range control requirements indicate that

the reentry vehicle should also have a mode:ate hypersonic lifting
capability (ref. 1). Studies currently beirg conducted by the NASA on
multimanned lunar-mission vehicles include a modified lenticular-shaped
configuration. The lenticular configuratior. fits the launching and
reentry requirements and is also capable of performing a flared horizon-
tal landing. The configuration reenters the earth's atmosphere in a
trimmed, high angle of attack, high drag, moderate lift condition.
Guidance corrections and impact range corrections are accomplished in
this condition. At transonic speeds, horizontal fins are extended to
trim the configuration to a low angle of attack, high lift condition.
Touchdown point selection and the horizonta:. landing maneuver are then
capable of being performed in this conditior. (refs. 2 to 4).

Recovery requirements indicate a need for the reentry vehicle to
have a capability of landing on land or sea. The "belly-landing" con-
cept discussed in reference 5 has possible application to the present
vehicle as a primary landing technique requiring little weight charge-
able to the landing system. A conventional flared landing would be made
with the curved lower surface of the vehicle (heat shield) serving as
a skid which would also convert sinking-speed energy into angular energy
in pitch (rocking oscillation) for dissipat:.on by friction and aero-
dynamic damping.

An application of this skid-rocker landing concept has been inves-
tigated on the lenticular vehicle. Impact acceleration and behavior
were determined with a free dynamic model landing on a hard-surface
runway over a range of landing attitudes and sinking speeds and on water
over a range of sea conditions. Auxiliary water landing gear, hydroskis,
and drag devices were briefly tested. A few vertical flight-path
landings (parachute letdown) were also made in calm water.

DESCRIPTION OF MODEL

The general arrangement of the 1/9-scale dynamic model is shown in
figure 1. Photographs of the basic model are shown in figure 2. Some
of the various landing-gear arrangements for water landings are shown
in figures 3 and 4. Figure 3(a) shows a hydroski attached directly to
the bow of the vehicle, whereas figure 3(b) shows a hydroski strut
mounted at the bow. Figure 3(c) shows a drag flap mounted on the vehi-
cle. In figure 4 are shown the approximate positions on the lower
vehicle surface of several spoiler arrangements tested. Full-scale and
model-scale relationships applicable to these tests are shown in table I.
Pertinent model and full-scale dimensions are given in table II.

The model had a circular-planform body with lenticular cross sec-
tions. It had a monocoque shell made up of several layers of fiber

glass and plastic and was reinforced internally by bulkheads in order to increase rigidity. The movable horizontal fins and end plates were made of lightweight fiber glass and plastic. In order to permit landing at roll attitudes, the lower end plates were given curvature, and the horizontal fins were held in position with a friction-clutch arrangement which permitted fin deflection under impact load. The initial-contact shock absorber (fig. 1) was a simple skid-lever mechanism which deformed a pure-nickel energy strap in tension with negligible spring effect. The shock absorber stopped the vertical motion of the effective mass at the point of first contact (near trailing edge) and permitted a smooth transition to rocking on the curved lower surface of the model.

APPARATUS AND PROCEDURE

The investigation was conducted by launching the model as a free body by use of the monorail apparatus of the Langley Research Center and landings were made on a hard-surface runway. (See fig. 5(a)). The catapult apparatus shown in figure 5(b) was used for landings in water. The hard-surface runway was constructed of a heavy wood decking covered with 1/2-inch plywood and supported on adjustable steel scaffolding mounted on the bottom of a tank of water. The landing surface was 8 feet wide and approximately 100 feet long with the end sloped into the water. When the model ran beyond the length of the runway provided, it was arrested by the water.

The horizontal fins were set for trimmed flight at the launching attitude and the model maintained approximately this attitude during free glide onto the landing surface. Initial contact was made at a nose-high attitude on the shock absorber at the trailing edge of the model. All landing tests were made at a model weight corresponding to a full-scale weight of 5,100 pounds.

The orientation of acceleration axes, force directions, attitudes, and flight path investigated are shown in figure 6. Hard-surface landings were made at a contact attitude of 30° (near maximum lift), a landing speed of 90 knots, and sinking speeds (vertical velocity) of 2 to 14 feet per second with a few landings made at a contact attitude of 20° and a landing speed of 110 knots (all values converted to full scale). These landing parameters were conditions expected at touchdown after flare-out. During the landings several touchdowns occurred with initial roll and yaw attitudes up to 15°. The sliding coefficient of friction during hard-surface landings was approximately 0.3.

The basic configuration was landed with and without auxiliary water-landing gear in calm water and in oncoming waves 2 to 7 feet high, full

4

scale (sea states 2 to 4) at a contact attitude of 30° and a landing
speed of 80 knots. A few landings were made at a 20° contact attitude
and a landing speed of 95 knots. The density of the water was 1.94 slugs
per cubic foot. The auxiliary water landing gear investigated included
hydroskis, spoiler strips, drag flaps, and a "dragline." Dragline
tests were made with the apparatus shown in figure 7. Desired values
of drag force were applied to the model during landing runout by a
constant-force drag reel. Exploratory calm-water landings were also
made with the basic configuration at reduced landing speeds (as low as
50 knots). A few vertical flight-path landings (90°) were made in calm
water by dropping the model as a free body from such a height as to
provide a vertical impact speed (full scale) of 70 feet per second.
Contact attitudes of -45° to -90° were investigated.

Longitudinal, normal, and angular accelerations at the vehicle
center of gravity were measured by strain-gage accelerometers rigidly
mounted to the model structure. Longitudinal and normal accelerations
were measured with a 15g and 20g accelerometer, respectively, and angular
acceleration was measured with a pair of matched 50g accelerometers. The
natural frequency was about 180 cycles per second for the 15g and 20g
accelerometers and about 310 cycles per second for the 50g accelerom-
eters. The accelerometers were damped to 65 percent of critical damping.
The response of the recording galvanometers was flat to about 190 cycles
per second for the 15g accelerometer and about 135 cycles per second
for the 20g and 50g accelerometers. Check tests during some of the
hard-surface landings were made with a galvanometer frequency of 20 cycles
per second. A trailing cable, propelled along an overhead guide wire,
was used to transmit accelerometer signals to an oscillograph recorder.
Motion-picture cameras located at the side of the towing tank and also
above and beyond the end of the runway recorded general behavior.

<div align="center">RESULTS AND DISCUSSION</div>

A short motion-picture film supplement of typical hard-surface and
water landings is available on loan from the NASA. A request card and
a description of the film will be found at the end of this paper. All
data presented are converted to full-scale values by use of the scale
relations given in table I.

<div align="center">Hard-Surface Landings</div>

Sequence photographs of typical landings of the model on the run-
way surface are shown in figure 8. The general behavior was very similar
for all hard-surface landings and was characterized by approach at a

high angle of attack (near maximum lift), touchdown on the trailing-edge shock absorber, transition to angular oscillation (rocking) along the lower surface of the vehicle, and the slide out during which angular oscillation was damped. During the first rocking oscillation the model rocked well forward to a nose-down attitude (approx. -30°).

Typical oscillograph records of acceleration during the hard-surface landings are shown in figure 9. High-frequency "hash" caused by irregularities between rigid sliding surfaces (model and runway) and by model vibrations were faired as shown in figure 9(a) in order to determine the acceleration values. Figure 9(b) shows results from a check test in which a recording galvanometer having a low-frequency response was used in order to eliminate hash and to define the rocking accelerations. During the skid-rocker landing, initial contact occurred at time A (fig. 9) after which initial sinking-speed energy at the trailing edge was absorbed by the shock absorber and rocking motion along the lower surface was initiated. The ground-contact point moved forward as the vehicle rocked forward so that a peak acceleration resulted at time B as the contact point passed below the center of gravity (approx. 0° attitude) and the vertical motion (fall) of the center of gravity was stopped. The ground contact point continued to move forward as the vehicle pitched to a nose-low attitude. When the stopping force (ground reaction) moved far enough forward to overcome the angular energy, the rocking motion was reversed. As the vehicle rocked back through 0° attitude another peak acceleration occurred at time C. Subsequent rocking oscillations (not shown in fig. 9) were progressively damped during slide out. The peak normal and angular accelerations obtained at times A, B, and C are shown in figure 10 for several landings at a contact attitude of 30° and various nominal initial sinking speeds. The maximum acceleration during landing always occurred at time B; that is, time at which the first rocker oscillation reached an attitude of 0°.

The maximum normal and angular accelerations during landing (at time B) are shown in figure 11 plotted against variation of initial sinking speed. Maximum normal acceleration increased slightly to approximately 5g and maximum angular acceleration increased from 10 to 18 radians per second^2 over a range of initial sinking speeds from 2 to 14 feet per second.

The normal and angular accelerations obtained at the three main points of the landing sequence for a few landings at a launch attitude of 20° and an initial sinking speed of 5 feet per second are shown in figure 12. However, as compared with landing at an attitude angle of 30° the data indicate some reduction in maximum normal acceleration and a substantial reduction in the maximum angular acceleration (see point at time B, fig. 10(b)). This reduction in acceleration was expected for the lower initial contact attitude because of the reduced rotational velocity acquired by the model at the time of peak acceleration

6

(when rocker contact point is below the center of gravity). The observed amplitude of the rocking oscillation was reduced as compared with that during landings at contact attitudes of 30°.

In general, the hard-surface landing characteristics of the model were considered good over a wide range of landing conditions. During several of the landings in which the model inadvertently landed at roll and yaw contact attitudes ranging to approximately 15°, directional stability during slide out was good. Maximum values of normal acceleration were unaffected, since the symmetry of the vehicle lower surface provided an unchanged rocker characteristic, regardless of the path of the rocking point with respect to the longitudinal axis.

Water Landings

Sequence photographs of typical landings of the model in calm water are shown in figure 13. Initial contact occurred on the trailing edge and the model immediately pitched down to a flat attitude, so that a sudden increase of wetted area resulted. At such high horizontal speeds a large restoring force was generated. This force, because of the body shape, resulted in an abrupt change in attitude along with large and erratic rebounds. The subsequent (second) impact frequently occurred at highly yawed, highly rolled, tail-first, or inverted contact attitudes. Overall behavior was quite similar but more pronounced during landings at a lower initial attitude (20°) due to increased horizontal landing speed. During landings in waves, rebounds or diving occurred depending on the sea conditions or the point of the wave contacted.

Typical oscillograph records of accelerations during landings in calm water and in waves are shown in figure 14. A small initial contact acceleration is immediately followed by the large first impact acceleration. Rebound is indicated by the long period between first and second impact. During rebound the model attained heights of 30 to 40 feet (full scale) above the water and very high pitch attitudes (70° to 90°). Considerable reduction of horizontal speed occurred during the rebound and the model dropped back to the water surface at steep flight-path angles with high sinking speed. The second impact was in all cases an impact with initial contact on the vehicle edge (circumference). Maximum longitudinal and normal accelerations during landing almost always occurred at first impact and maximum angular acceleration was about evenly divided between first and second impact. Third impacts, when they did occur, were insignificant.

The maximum accelerations obtained during horizontal landings in water with the basic configuration are shown in figure 15 for sea conditions varying from calm water to a wave height of 7 feet, representative of sea state 4. In general, accelerations increased with increase

in wave height. In going from calm water to 7-foot waves maximum lon-
gitudinal accelerations increased from approximately 5g to 10g, normal
accelerations from 9g to 21g, and angular accelerations from 65 to
145 radians per second^2. An increase in initial sinking speed for the
calm-water case resulted in increased normal and angular acceleration.

It was observed that during some of the landings in waves the model
made initial contact near the crest of a wave and trimmed down to a
fairly flat attitude at first impact on the advancing slope of the next
wave. Study of motion pictures of landings in the 7-foot wave revealed
a first impact which occurred near midslope of the wave at a vehicle
attitude equal to the maximum theoretical wave slope (approx. 10°). On
the assumption that at impact the sinking speed was small and horizontal
speed relatively unchanged (only slightly below contact speed) the veloc-
ity vector normal to the wave surface could be determined and normal
acceleration could be computed by the method of reference 6. The vehicle
velocity normal to the wave surface at impact was approximately 25 feet
per second (sinking speed being ignored) and the computed peak accelera-
tion was 23g, which compares favorably with the measured value of 21g.
Figure 16 shows computed acceleration time histories and peak accelera-
tions for various impact velocities normal to the water surface at a
vehicle contact attitude of 0° relative to the water surface.

Maximum accelerations obtained during landings with the bow attached
hydroski are shown in figure 17. As expected, normal and angular accel-
erations are less than those obtained for the basic model. Increase in
wave length resulted in decreased accelerations to a value, in a very
long wave, near that for calm water. However, the hydroskis tested were
not adequate to improve the overall behavior characteristics significantly.
General behavior in waves was similar to that of the basic vehicle; how-
ever, improved landing characteristics were noted during landing in calm
water at low initial sinking speeds.

A summary of results obtained during brief water-landing tests of
the model with drag devices is presented in table III. In general,
results show little significant improvement and in some cases behavior
worsened (for example, tumbling occurred). However, dragline tests
indicated that improvement might be realized with drastic reduction of
landing speed. During exploratory calm-water landings of the basic con-
figuration at reduced landing speeds and 30° contact attitude landing
motions improved as speed was reduced. At the lowest speed of the tests,
approximately 50 knots, rebound was slight. Such a landing would require
a braking force (rocket or drogue-chute) and positive control over con-
tact attitude as well as initial sinking speed.

Typical oscillograph records of acceleration during vertical landings
(simulated parachute letdown) on calm water are shown in figure 18 and
maximum accelerations are shown in figure 19. During all landings the

model submerged and changed attitude while submerged, surfacing in an upright position. Submergence was deep for the -90° contact attitude but shallow for the other attitudes tested. As the flatness of the impact was increased (contact attitude going from -90° to -45°) the maximum longitudinal acceleration increased from approximately 5g to 9g, normal acceleration from 3g to 15g, and angular acceleration from 10 to 110 radians per second².

CONCLUDING REMARKS

Hard-surface landing characteristics of a lenticular-shaped reentry vehicle obtained with the curved lower surface (heat shield) used as a skid-rocker were good and resulted in maximum normal and angular accelerations of 5g and 18 radians per second², respectively, over a range of landing conditions. Horizontal landings in water resulted in large and violent rebounds or dives, depending on the sea conditions or the point of the wave contacted. The nature of the rebounds was such that the attitude of subsequent impacts was random. The maximum longitudinal accelerations obtained in water landings were 10g, maximum normal accelerations were 21g, and maximum angular accelerations were 145 radians per second² in waves 7 feet high (sea state 4). Various auxiliary water-landing devices tested produced no practical improvement in behavior. Reduction of horizontal speed and positive control of impact attitude did improve performance in calm water. During vertical landings (90° flight path) in calm water maximum longitudinal accelerations were 9g, maximum normal accelerations were 15g, and maximum angular accelerations were 110 radians per second² for a contact attitude of -45° and a vertical velocity of 70 feet per second.

Langley Research Center,
    National Aeronautics and Space Administration,
        Langley Field, Va., June 13, 1961.

REFERENCES

1. Staff of Langley Flight Research Division (Compiled by Donald C. Cheatham): A Concept of a Manned Satellite Reentry Which is Completed with a Glide Landing. NASA TM X-226, 1959.

2. Ware, George M.: Static Stability and Control Characteristics at Low-Subsonic Speeds of a Lenticular Reentry Configuration. NASA TM X-431, 1960.

3. Mugler, John P., Jr., and Olstad, Walter B.: Static Longitudinal Aerodynamic Characteristics at Transonic Speeds of a Lenticular-Shaped Reentry Vehicle. NASA TM X-423, 1960.

4. Jackson, Charlie M., Jr., and Harris, Roy V., Jr.: Static Longitudinal Stability and Control Characteristics at a Mach Number of 1.99 of a Lenticular-Shaped Reentry Vehicle. NASA TN D-514, 1960.

5. Mayo, Wilbur L.: Skid Landings of Airplanes on Rocker-Type Fuselages. NASA TN D-760, 1961.

6. McGehee, John R., Hathaway, Melvin E., and Vaughn, Victor L.: Water-Landing Characteristics of a Reentry Capsule. NASA MEMO 5-23-59L, 1959.

TABLE I.- SCALE RELATIONSHIPS

$$\left[\lambda = \text{Scale of model}\right]$$

Quantity	Full scale	Scale factor	Model
Length	l	λ	λl
Area	A	λ^2	$\lambda^2 A$
Weight	w	λ^3	$\lambda^3 w$
Moment of inertia	I	λ^5	$\lambda^5 I$
Time	t	$\sqrt{\lambda}$	$\sqrt{\lambda}\,t$
Speed	v	$\sqrt{\lambda}$	$\sqrt{\lambda}\,v$
Linear acceleration . . .	a	1	a
Angular acceleration . . .	α	λ^{-1}	$\lambda^{-1}\alpha$
Force	F	λ^3	$\lambda^3 F$

TABLE II.- PERTINENT DIMENSIONS OF LENTICULAR REENTRY VEHICLE

	1/9-scale model	Full scale
General:		
Gross weight, lb	7.0	5,100
Moment of inertia (approx.):		
Roll, slug-ft^2	0.025	1,450
Pitch, slug-ft^2	0.052	3,070
Yaw, slug-ft^2	0.070	4,140
Body:		
Length, ft	1.44	13.0
Planform area, sq ft	1.63	132.7
Fins:		
Horizontal-fin area (each), sq ft . .	0.316	25.6
End-plate area (each), sq ft	0.112	9.7
Hydroski (bow attached):		
Length, ft	0.67	6.00
Beam, ft	0.08	0.75
Surface area, sq ft	0.05	4.07
Step ahead of center		
of gravity, ft	0.08	0.75
Step below center of gravity, ft . . .	0.42	3.75
Incidence, deg	35	35
Hydroski (strut mounted):		
Length, ft	0.42	3.75
Beam, ft	0.15	1.31
Surface area, ft	0.46	4.10
Step ahead of center		
of gravity, ft	0.25	2.25
Step below center of gravity, ft . . .	0.50	4.50
Incidence, deg	11	11

TABLE III.- SUMMARY OF RESULTS OF LANDINGS IN WATER WITH VARIOUS DRAG DEVICES

[Contact attitude, approximately 30°; gross weight, 5,100 lb; landing speed, 80 knots; wave height, 3.5 ft; wave length, 200 ft. Motions determined from several test runs; accelerations measured during one test run. All values full scale.]

Configuration	Description	Sea condition	Maximum acceleration[1]			Motions
			a_1	a_2	a_3	
Spoiler strips (flow interrupter)	Cross section, 45° wedge Depth, 1⅛ in. Variations: length, location, arrangement	Calm				No significant effect noted, motions similar to basic configuration
Drag flap (0.75-ft beam)	Location, lower surface at trailing edge Length, 2.62 ft Surface area, 1.55 sq ft Angle, -50° (leading edge down)	Calm	7	10.5	100	Rebound, similar to basic configuration
		Wave	8 7	9 -22	80 55	Rebound Tumble
Drag flap (0.94-ft beam)	Location, lower surface at trailing edge Length, 2.62 ft Surface area, 1.93 sq ft Angle, -50°	Calm	6.5	11.5	70	Rebound
		Wave	6.5	-15	-60	Tumble
	Location, lower surface beneath ... Angle, -30°	Calm	5.5	9.5	55	Smooth runout, slight rebound near end
		Wave	8.5	-14 10	-60 105	Tumble Rebound
Drag flap (1.5-ft beam)	Location, lower surface at trailing edge Length, 2.62 ft Surface area, 3.1 sq ft Angle, -50°	Calm	8.5	8	85	Sudden stop and dive at first contact
Dragline simulator (above water)	Drag force applied at trailing edge by dragline Force varied with stationary drag reel Approximate forces applied: 700, 1,400, 2,000 lb	Calm				Improved braking, slightly reduced rebound, undesirable nose-down pitch motion during rebound (induced by attachment point and amount of drag force)

1 a_1 longitudinal acceleration, g units
a_2 normal acceleration, g units
a_3 angular acceleration, radians per sec²
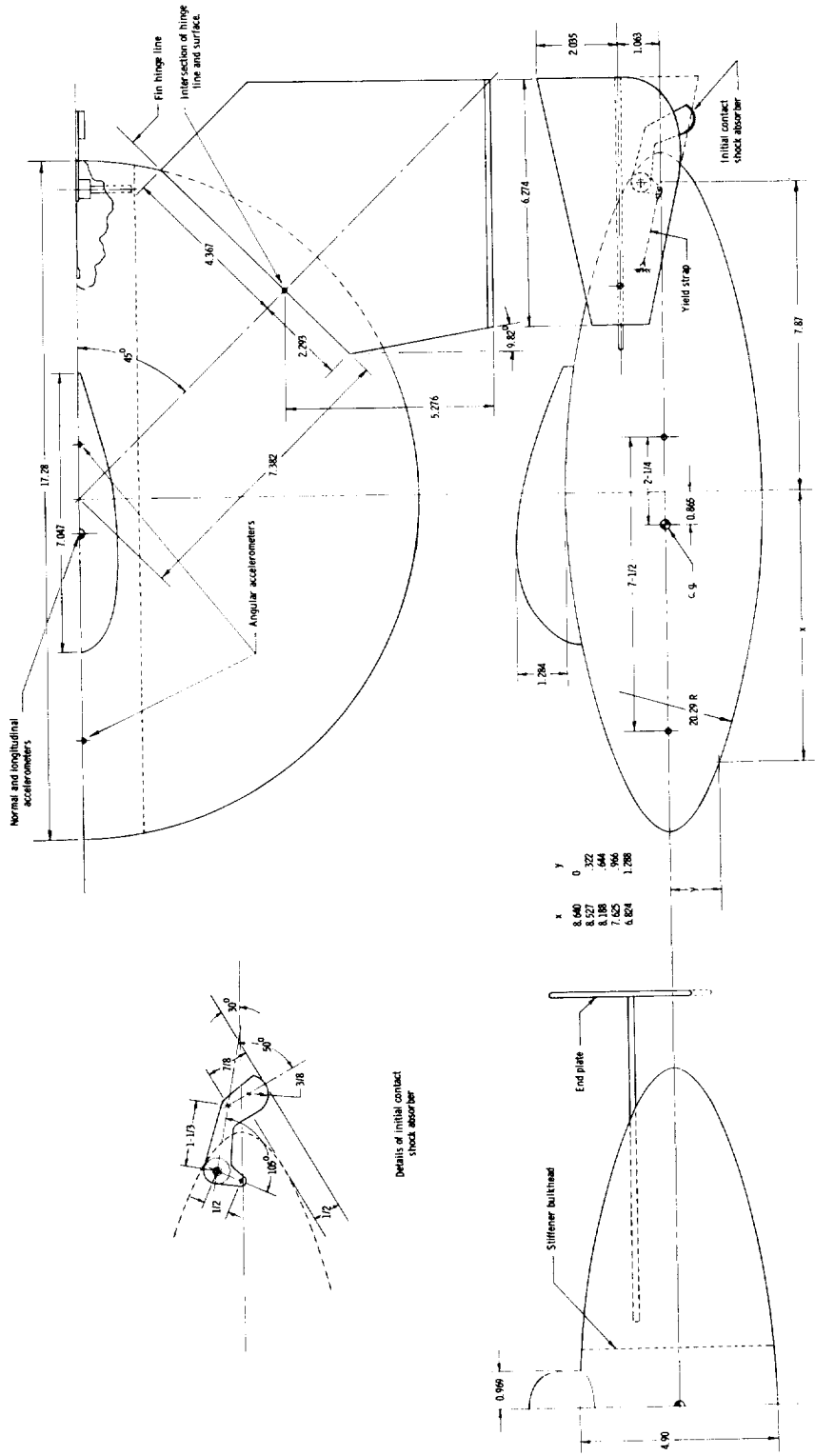
L-1676

Figure 1.- General arrangement of 1/9-scale dynamic model of the lenticular reentry vehicle. All dimensions are in inches. Model scale.

14
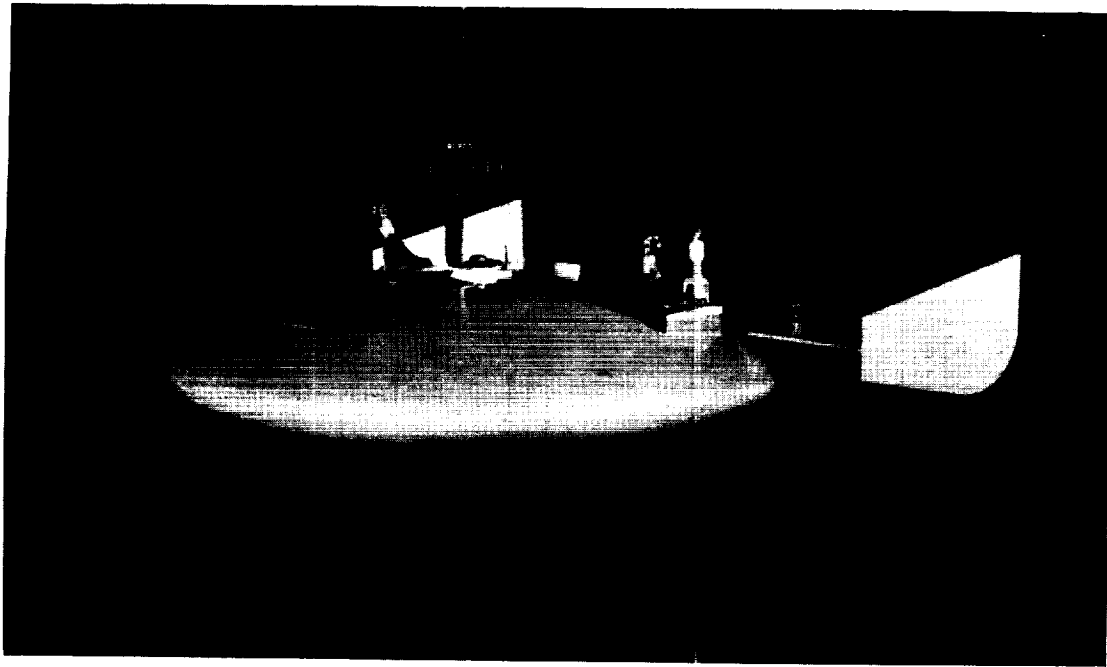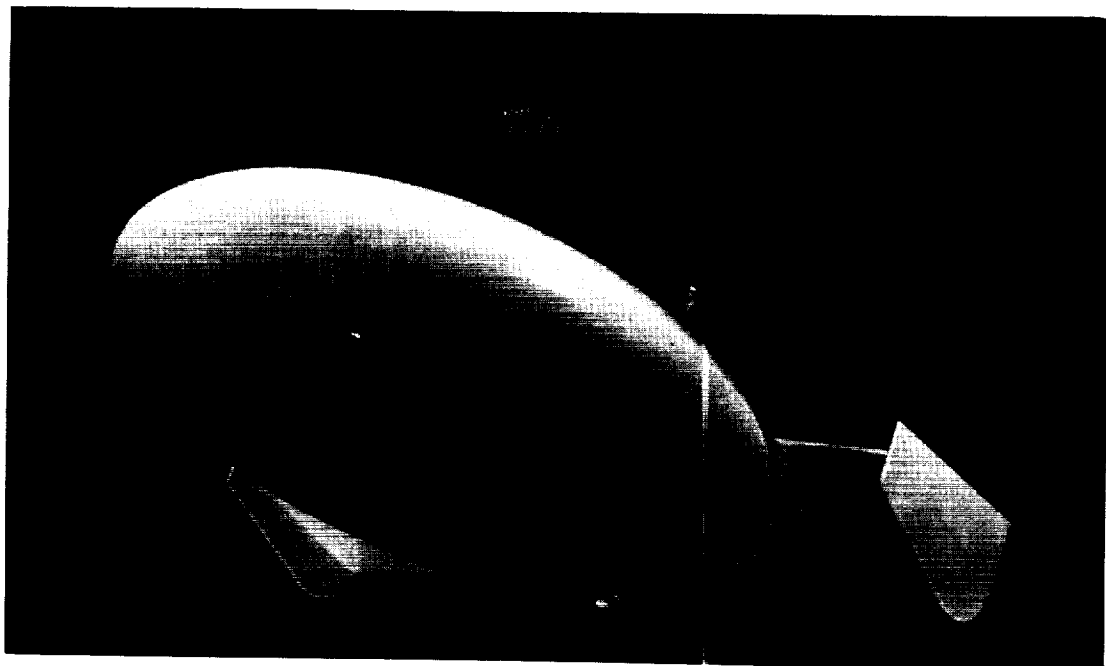
L-60-6000

Figure 2.- Photographs of basic model.   L-60-6004

L-1676
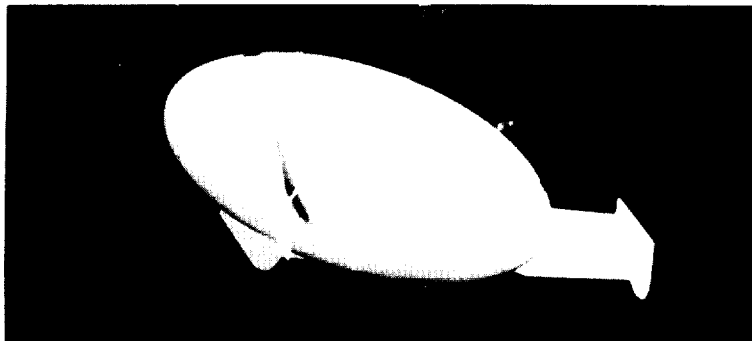
L-1676

(a) Hydroski (bow attached).   L-61-1432
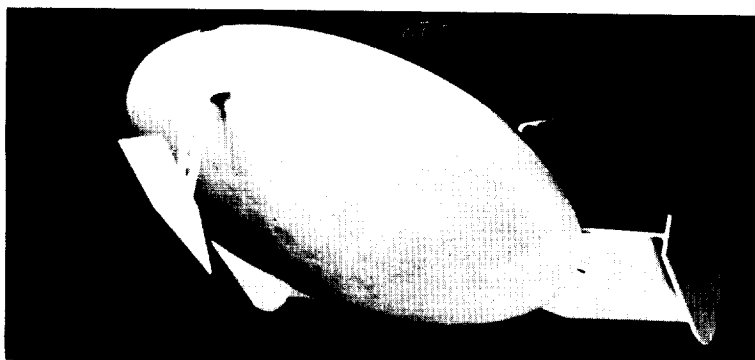
(b) Hydroski (strut mounted).   L-61-1431
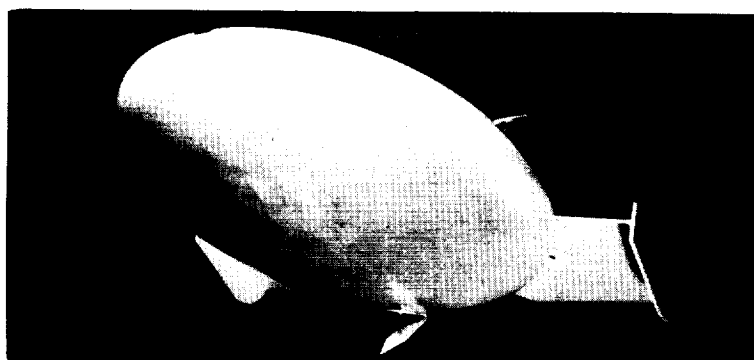
(c) Drag flap.   L-61-1428

Figure 3.- Photographs showing hydroskis and a drag flap installed on model.

Forward
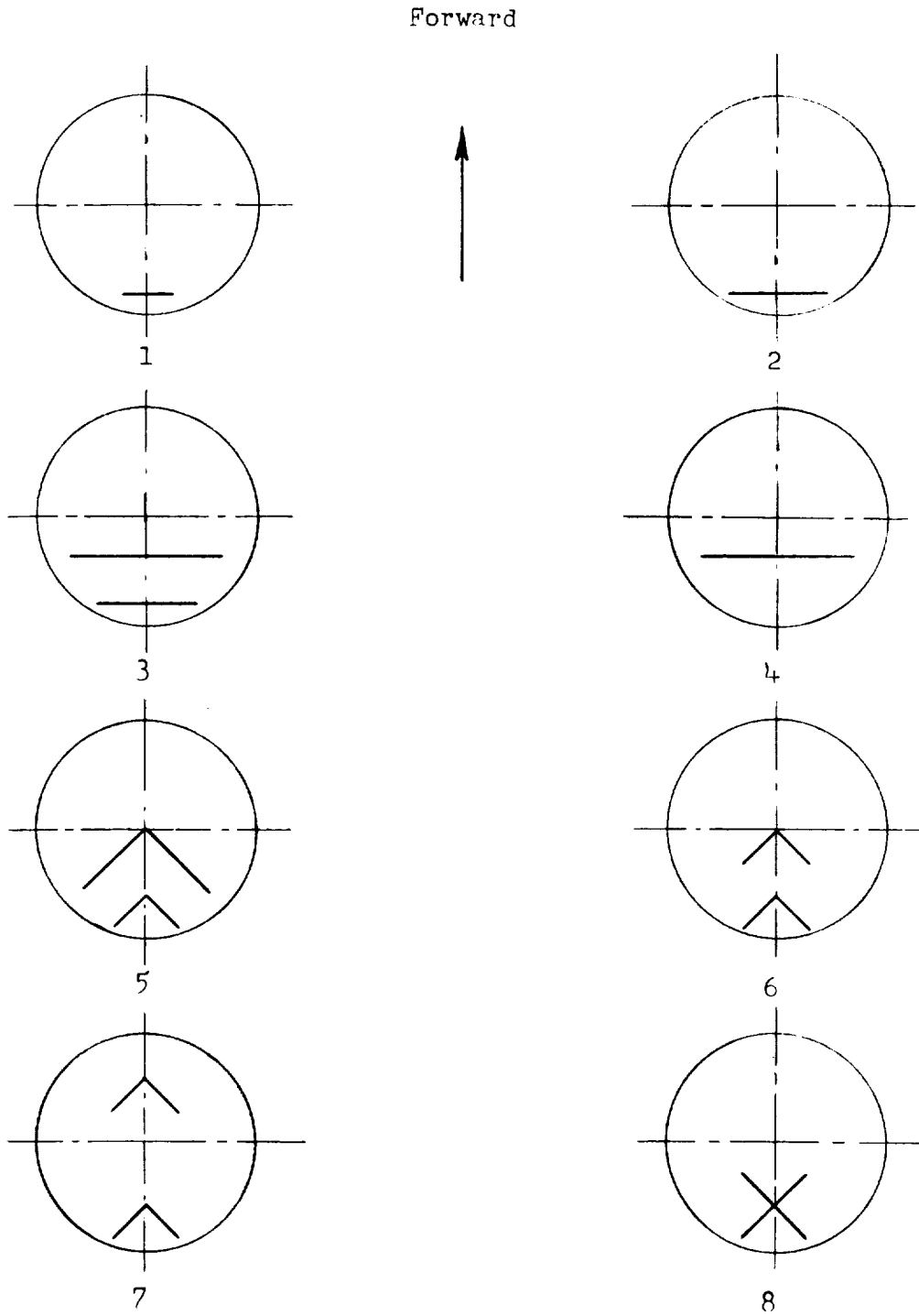
Figure 4.- Sketches showing various spoiler strip arrangements and approximate location on model lower surface.

L-1676

L-60-5998.1

(a) Monorail and runway.

Figure 5.- Photographs of test facilities.

18

Instrument cable

Recorder

Launching carriage

Catapult

Model
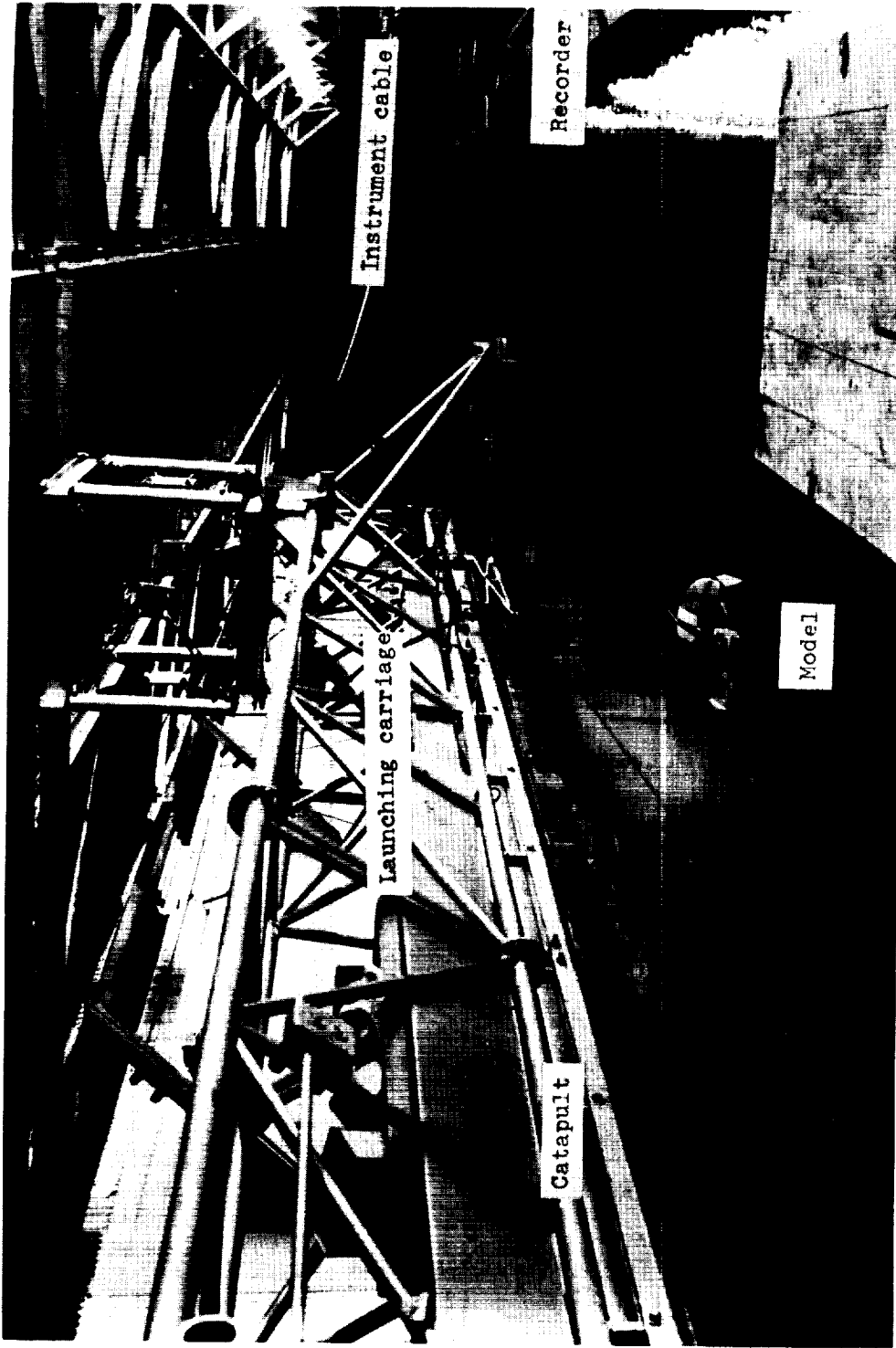
L-61-878

(b) Catapult.

Figure 5.- Concluded.
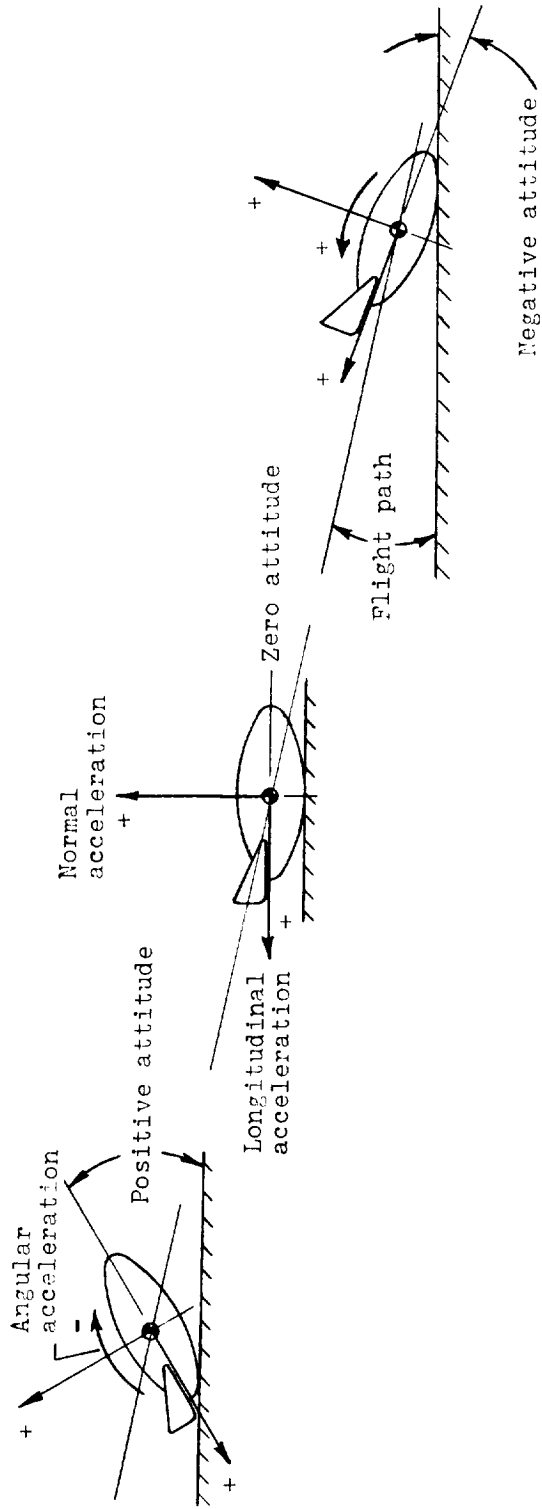
L-1676

L-1676

Figure 6.- Sketches identifying acceleration axes, attitudes, force directions, and flight path.

20

Carriage bumper

Catapult carriage

Catapult rail

Drag reel
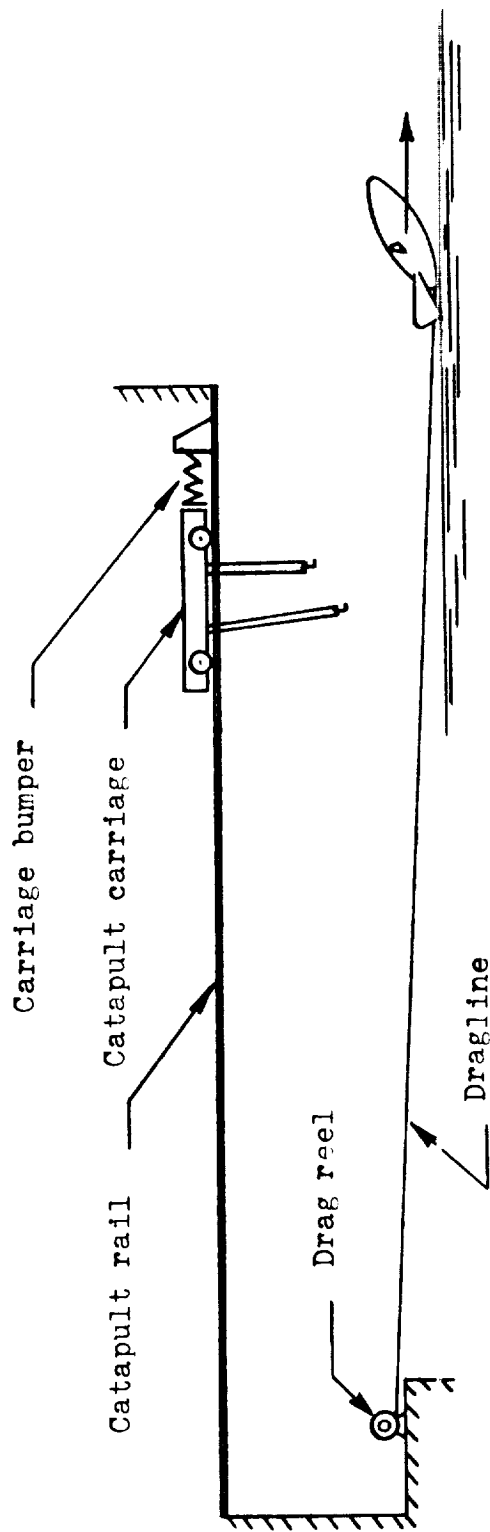
Dragline

Figure 7.- Sketch showing dragline test setup.

L-1676

L-1676

1

2

3

4

5

6

7

8
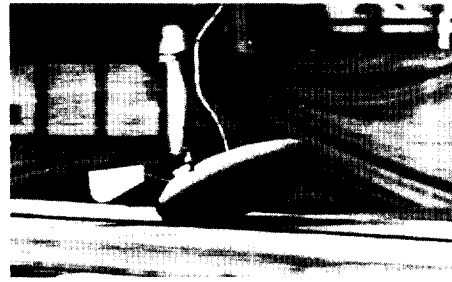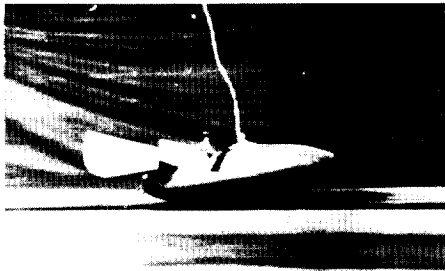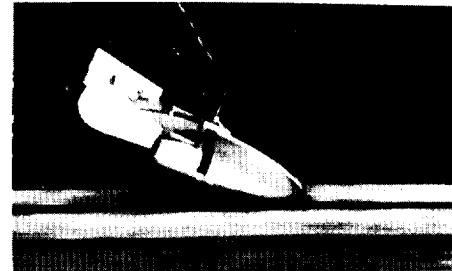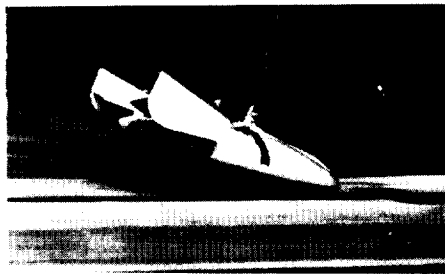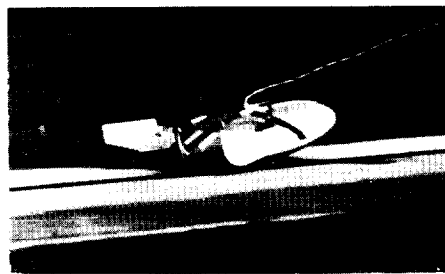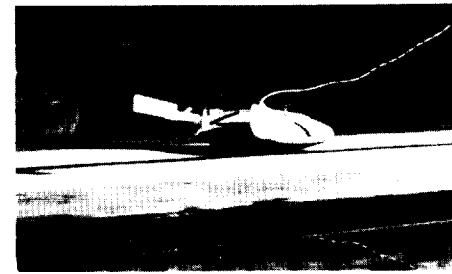
L-60-7694.1

Figure 8.- Sequence photographs during typical landing of basic model on
hard-surface runway.
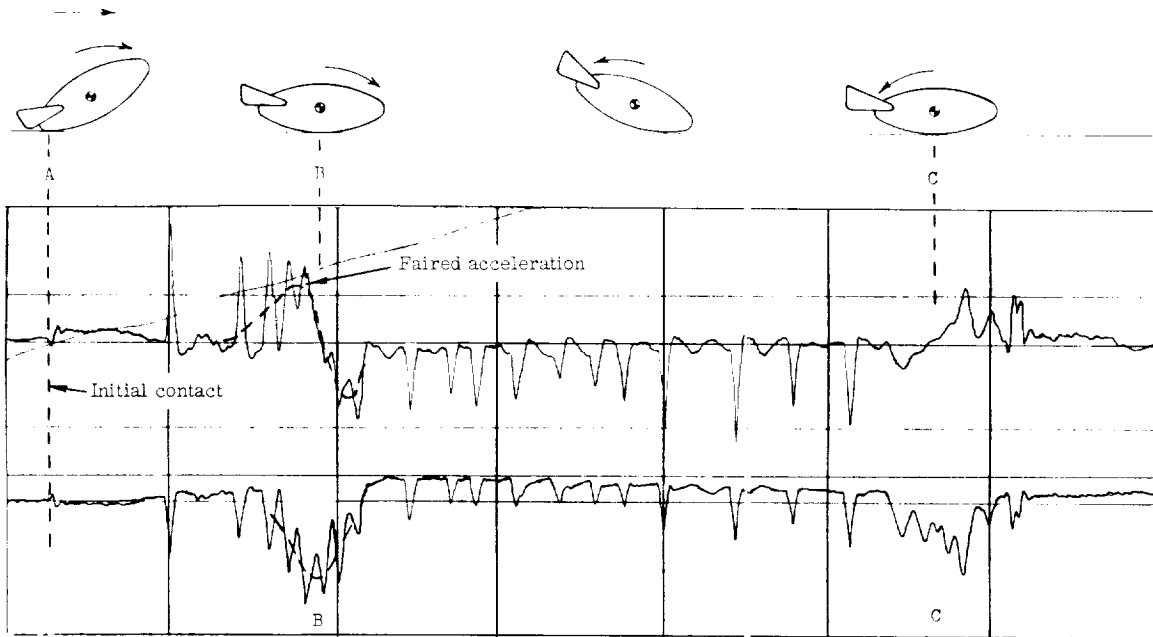
(a) High-frequency galvanometer.
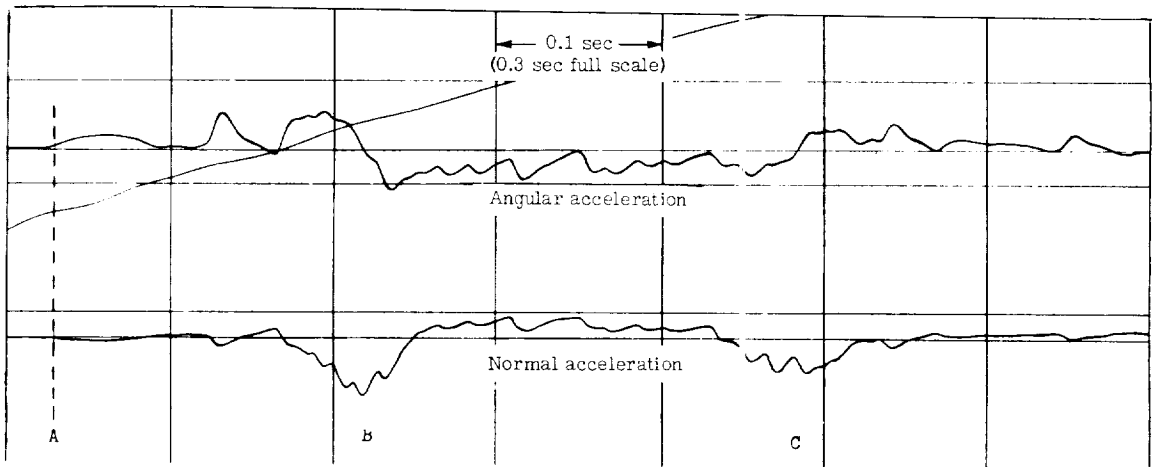
(b) Low-frequency galvanometer.

Figure 9.- Typical oscillograph records of accelerations during horizontal landings on hard surface.

L-1676
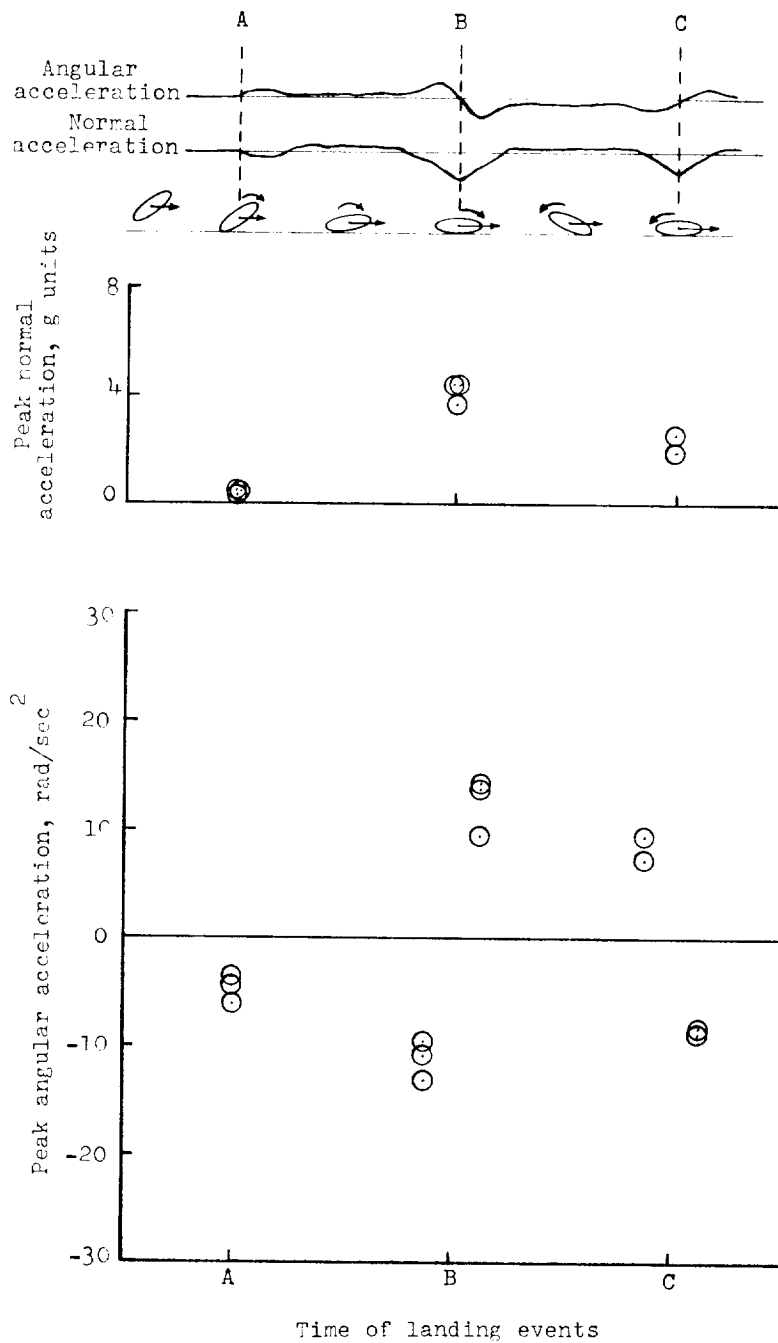
(a) Nominal initial sinking speed, 2 feet per second.

Figure 10.- Peak accelerations obtained at initial contact and during rocking motions in landings on hard-surface runway. Contact attitude, 30°; gross weight, 5,100 pounds; landing speed, 90 knots.
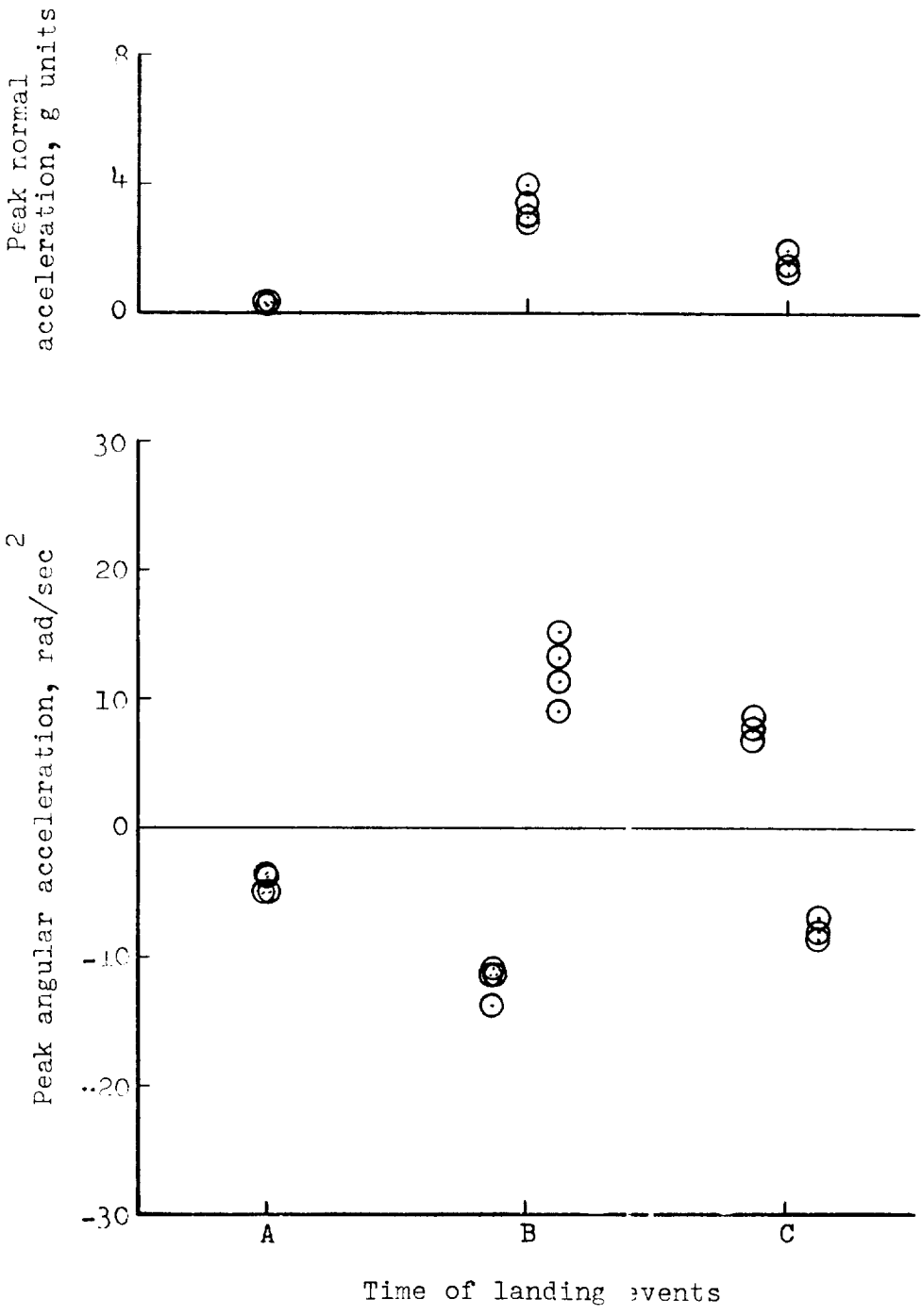
(b) Nominal initial sinking speed, 5 feet per second.

Figure 10.- Continued.
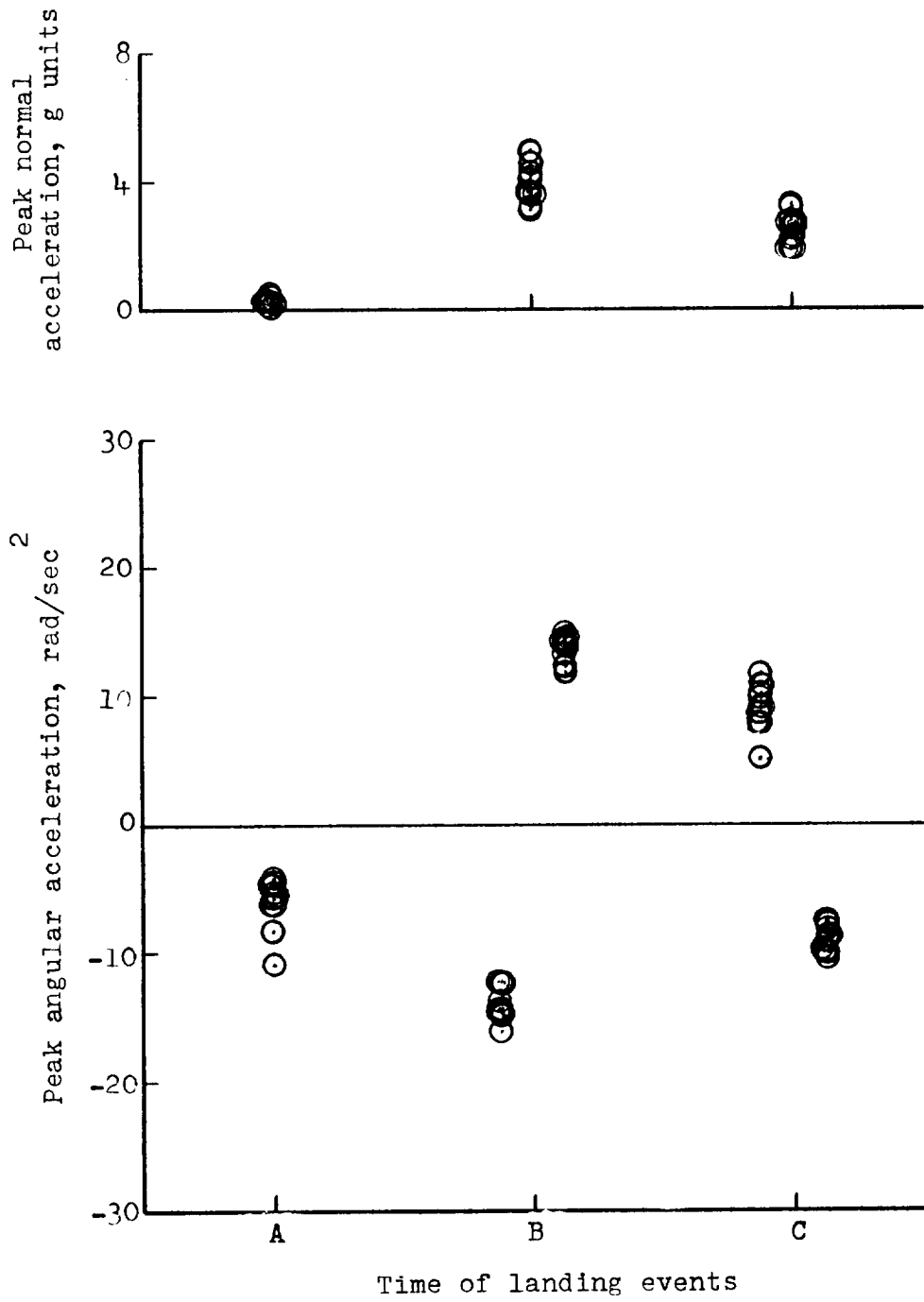
(c) Nominal initial sinking speed, 8 feet per second.

Figure 10.- Continued.
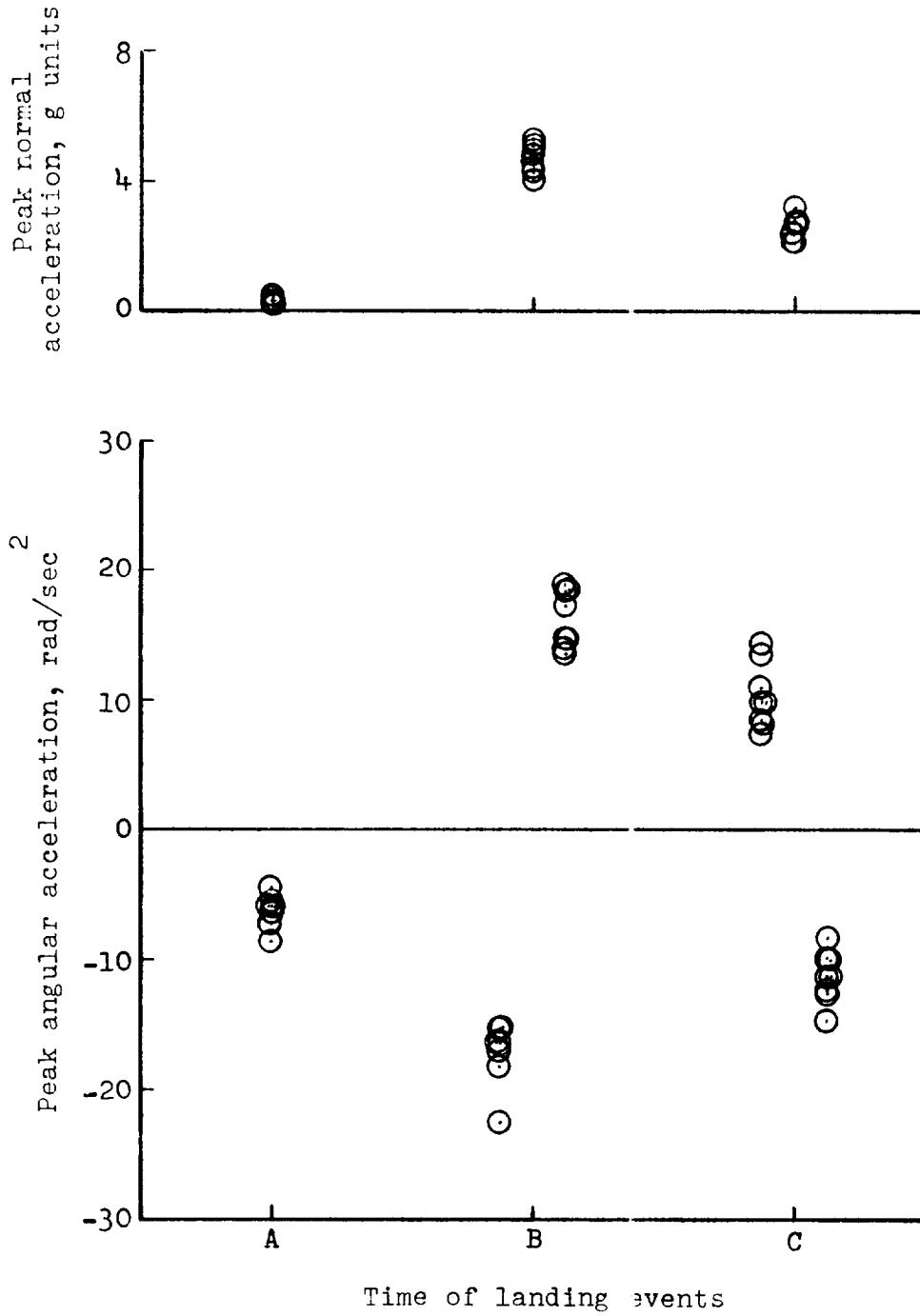
(d) Nominal initial sinking speed, 11 feet per second.

Figure 10.- Concluded.

L-1676
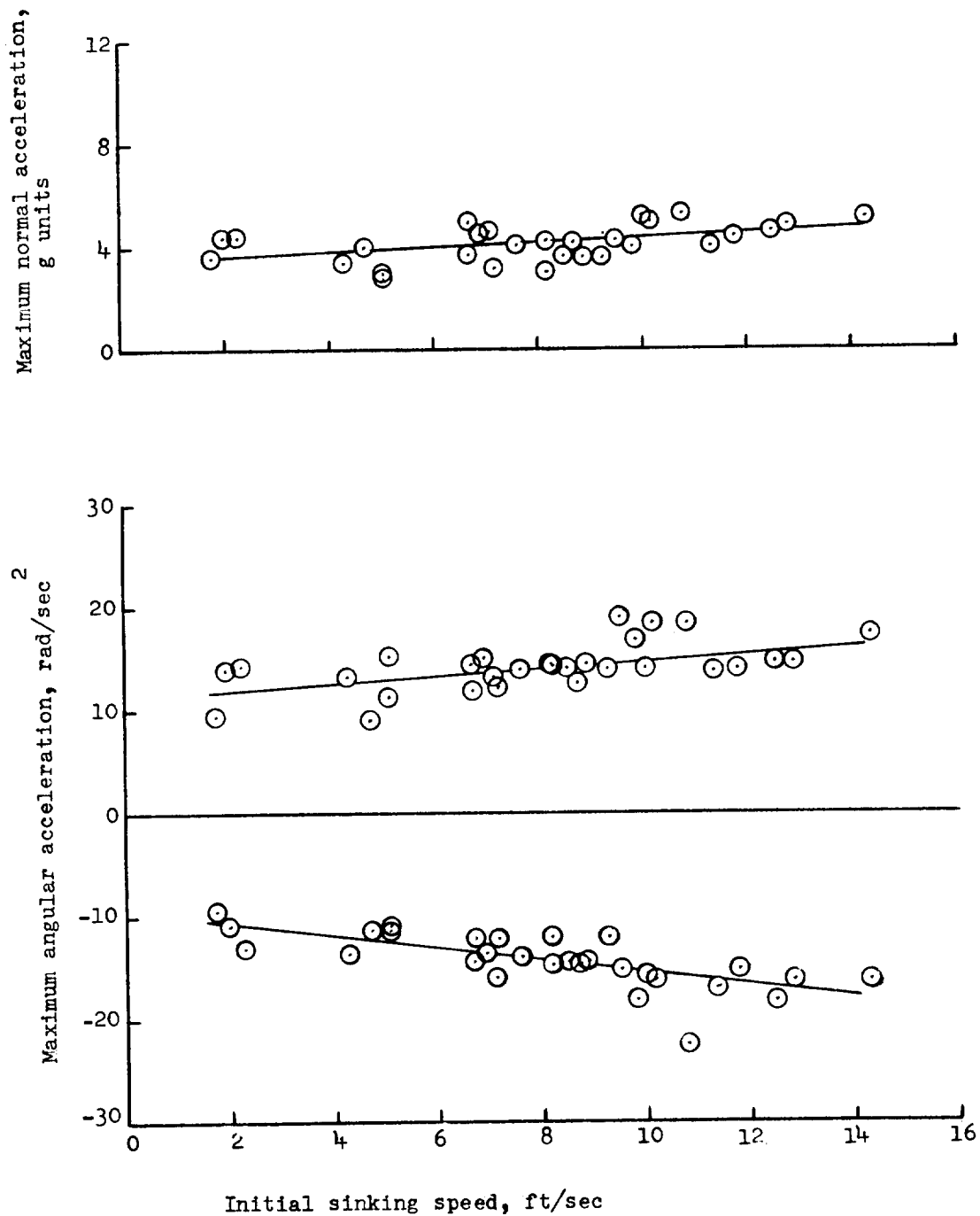
Figure 11.- Maximum accelerations at time B, obtained during landings on hard-surface runway for various initial sinking speeds. Contact attitude, 30°; gross weight, 5,100 pounds; landing speed, 90 knots.
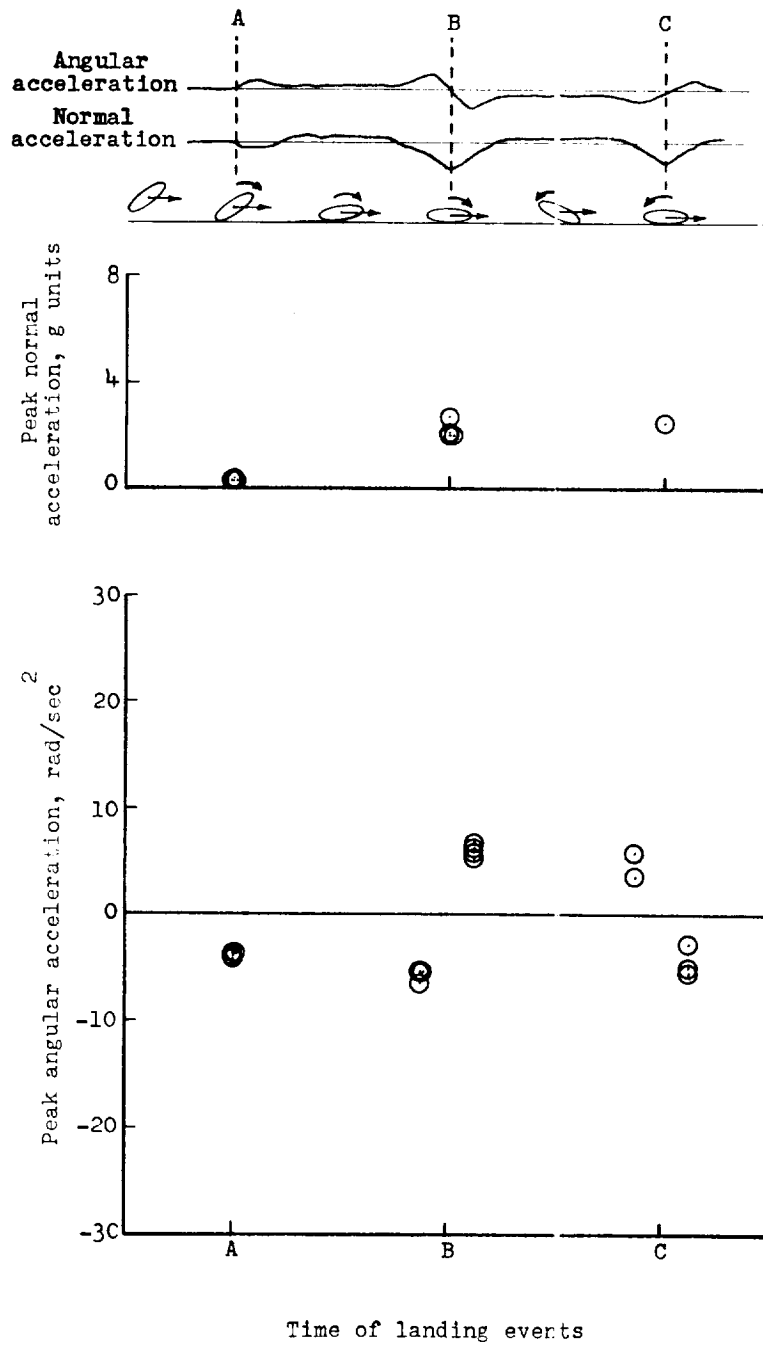
Figure 12.- Peak accelerations obtained at initial contact and during rocking motions in landings on hard-surface runway. Contact attitude, 20°; gross weight, 5,100 pounds; landing speed, 110 knots; initial sinking speed, 5 feet per second.

L-1676
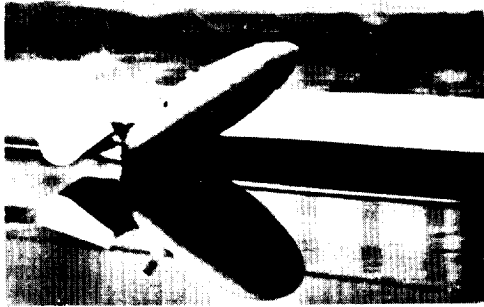
1

2

3

4
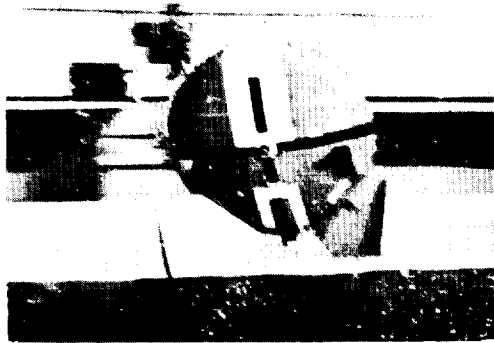
5

6

L-61-2102

Figure 13.- Sequence photographs during typical landing of basic model in calm water.

30

Longitudinal acceleration

Angular acceleration

Normal acceleration

Initial contact

1st impact

2nd impact

0.1 sec
(0.3 sec full scale)
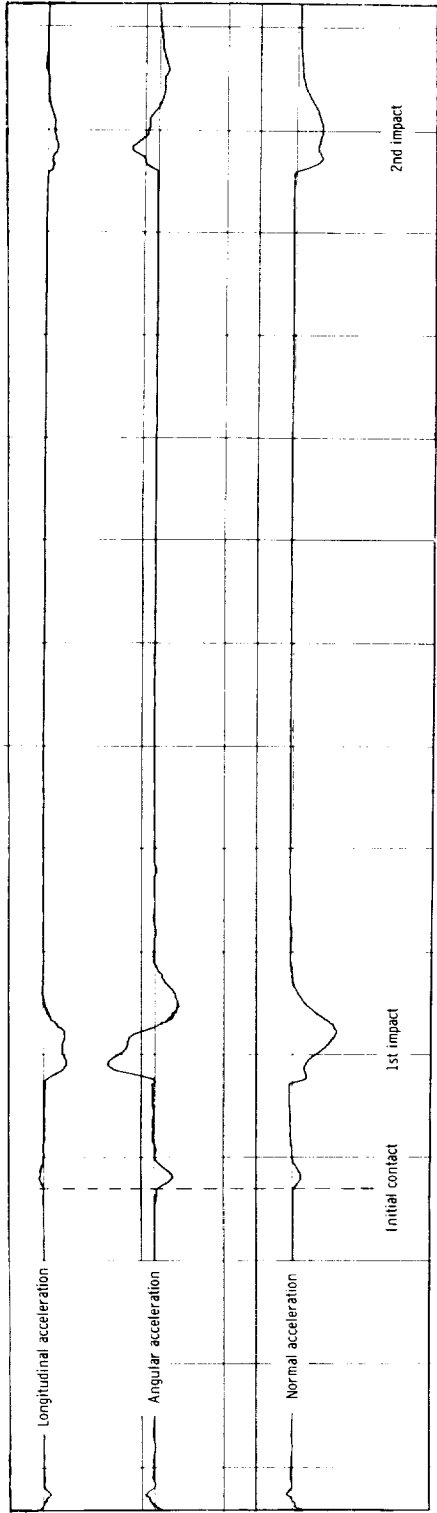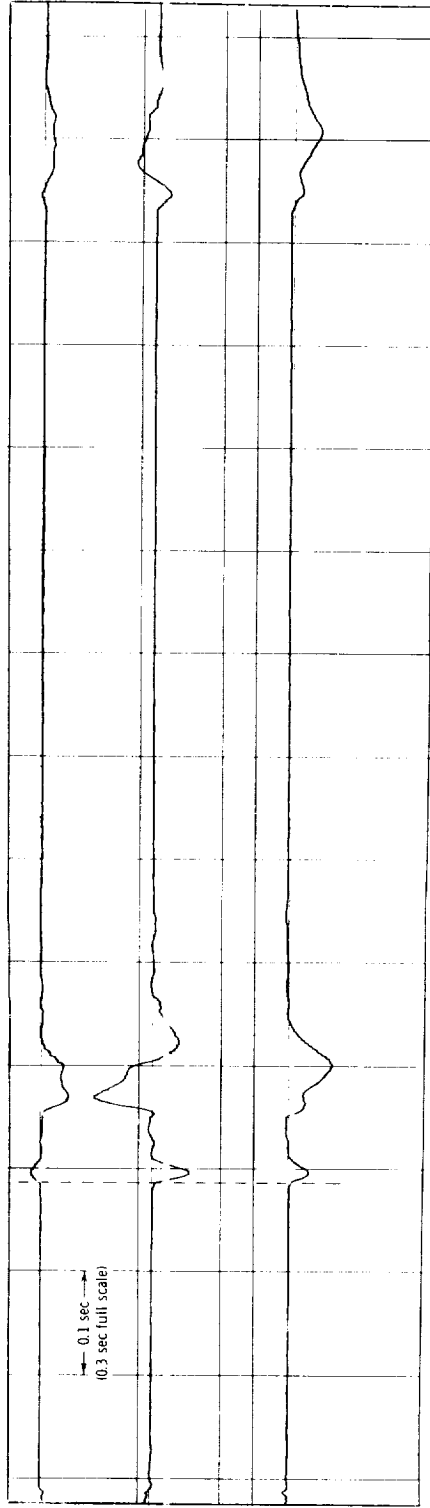
(a) Calm water.

(b) Waves.

Figure 14.- Typical oscillograph records of accelerations during horizontal landings in water.
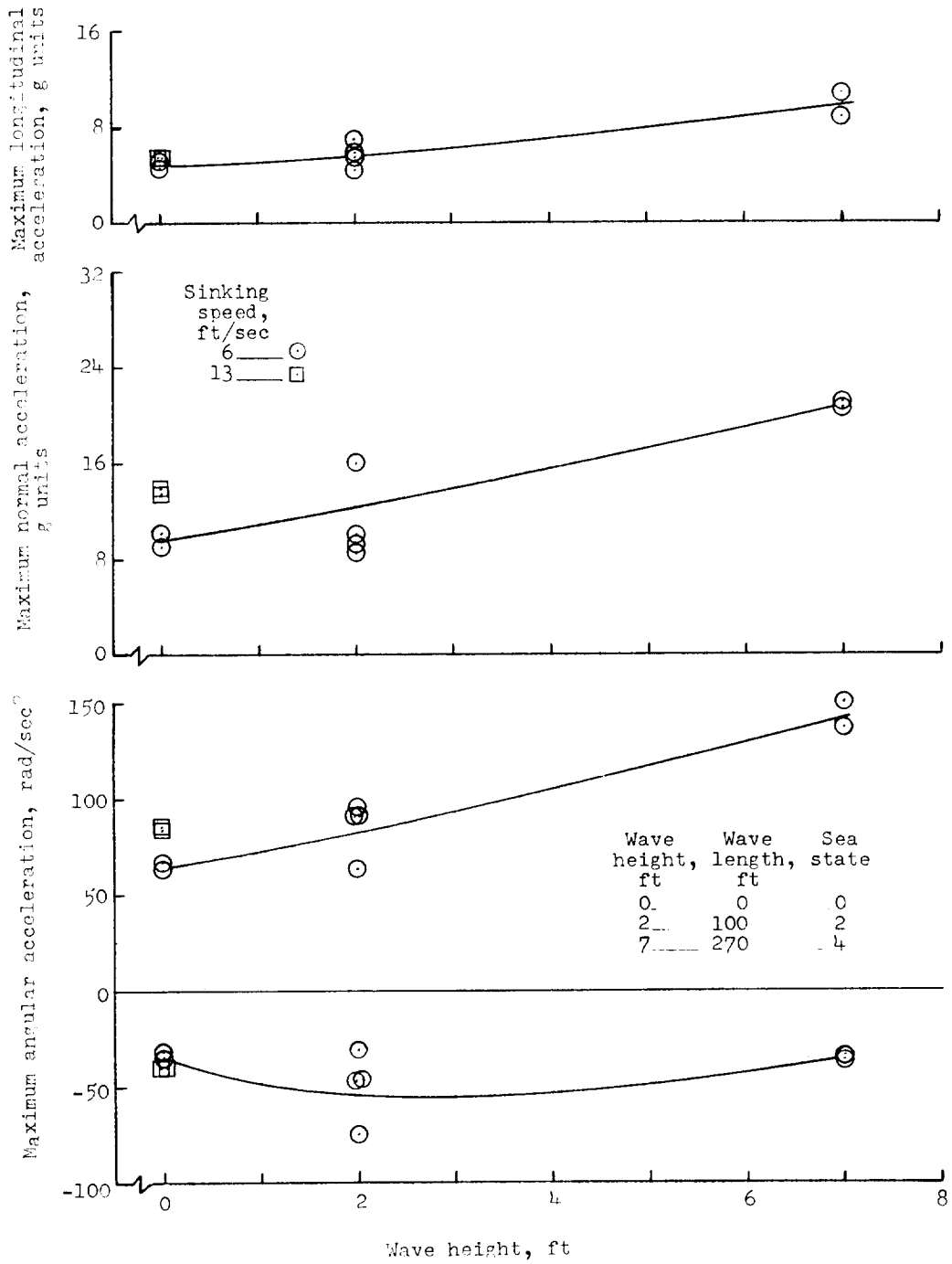
Figure 15.- Maximum accelerations obtained during horizontal landings in calm water and waves. Basic configuration; contact attitude, 30°; gross weight, 5,100 pounds; landing speed, 80 knots.

32
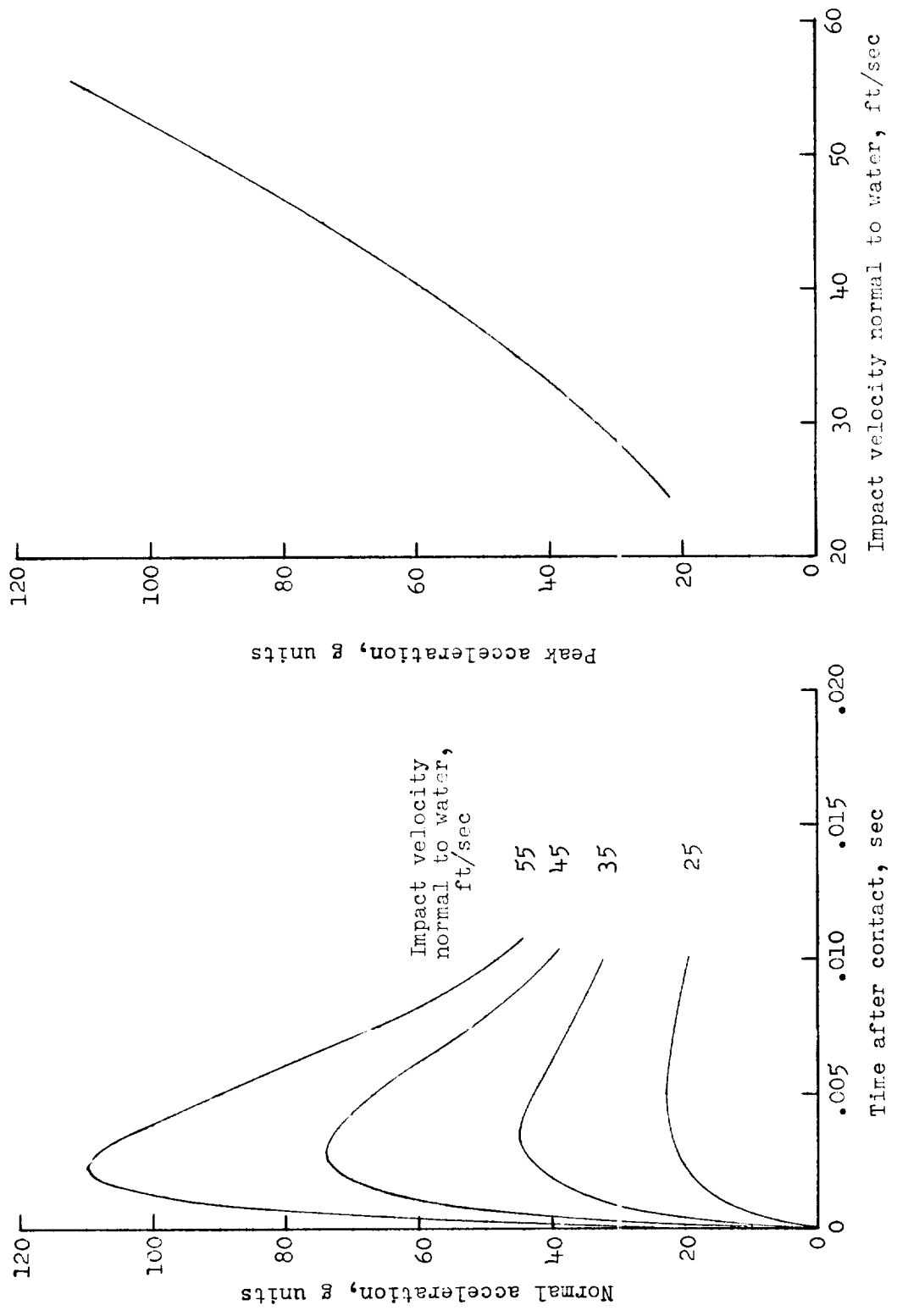
Figure 16.- Computed time histories and peak values of normal acceleration of basic configuration for various impact velocities normal to water surface at contact attitude of 0°.

L-1676

L-1676

Maximum longitudinal acceleration, g units

16

8

0

Basic configuration
with hydroski ————
Basic configuration ————

Maximum normal acceleration, g units

32

24

16

8

0

Wave   Sea
height, state
ft
0 ——— 0
2 ——— 2
4 ——— 3

Wave length,
ft

○ 100
⊞ 200
△ 315

Maximum angular acceleration, rad/sec²

150

100

50

0

-50

-100

0   2   4   6   8

Wave height, ft
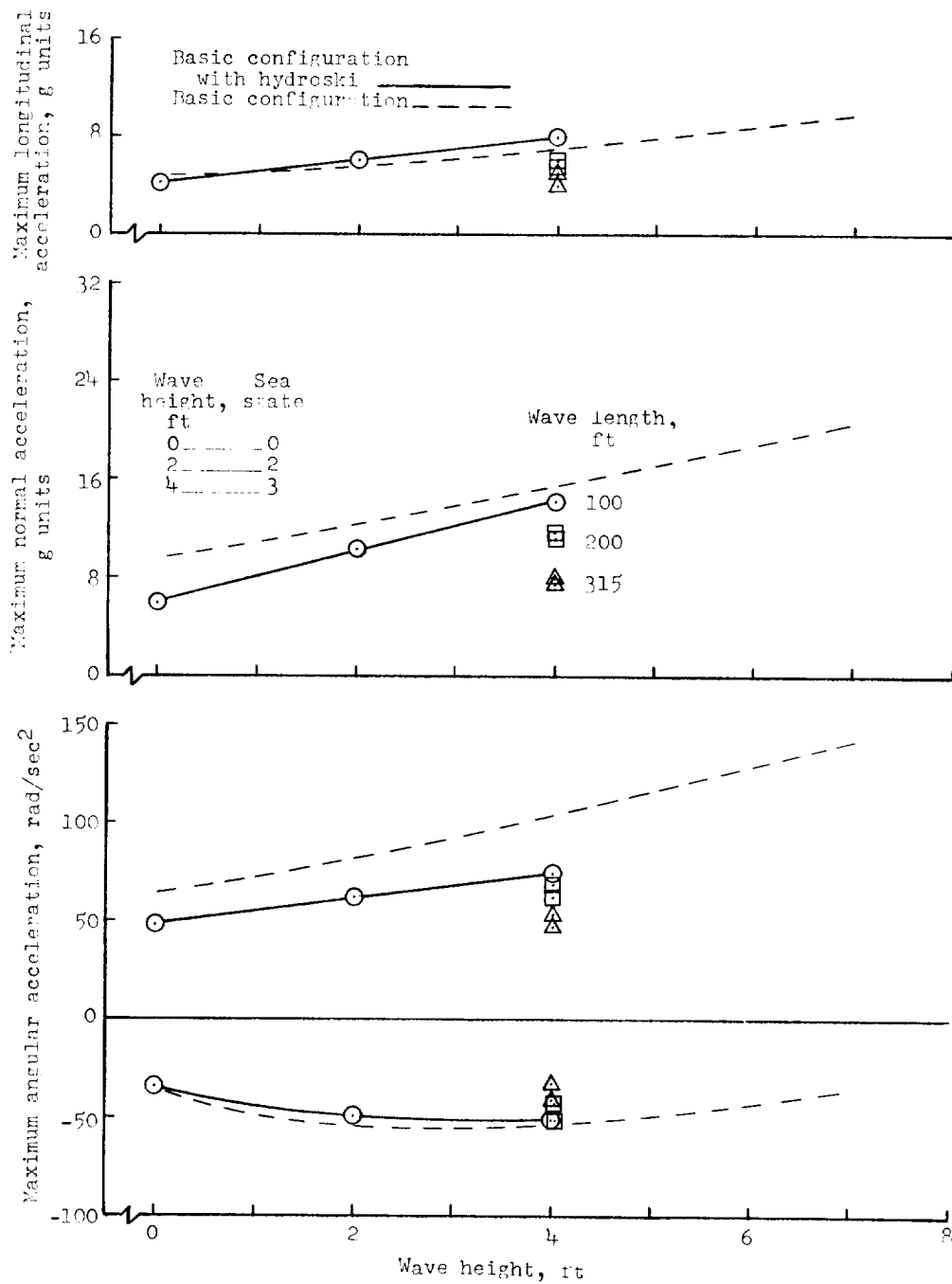
Figure 17.- Maximum accelerations obtained during horizontal landings in
calm water and waves. Basic configuration with bow-attached hydroski;
contact attitude, 30°; gross weight, 5,100 pounds; landing speed,
80 knots.
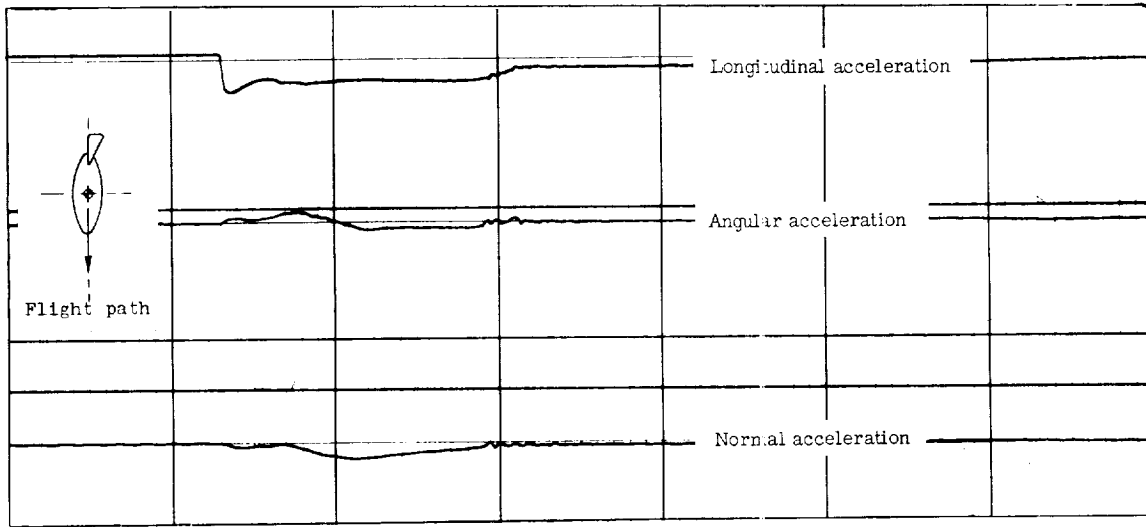
(a) Contact attitude, -90°.
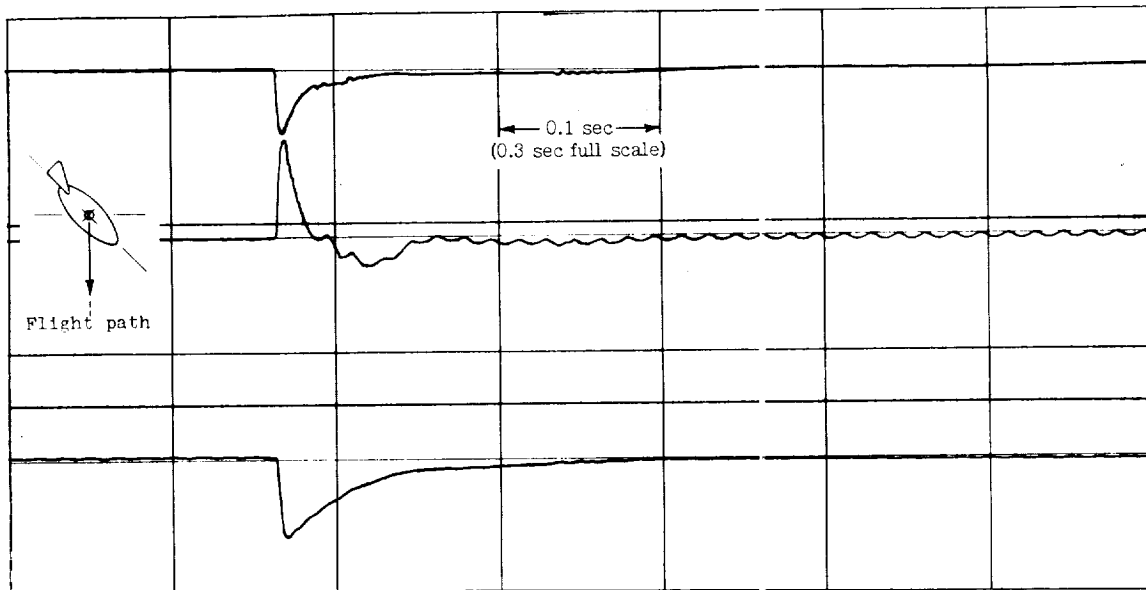
(b) Contact attitude, -45°.

Figure 18.- Typical oscillograph records of accelerations during vertical landings in water.
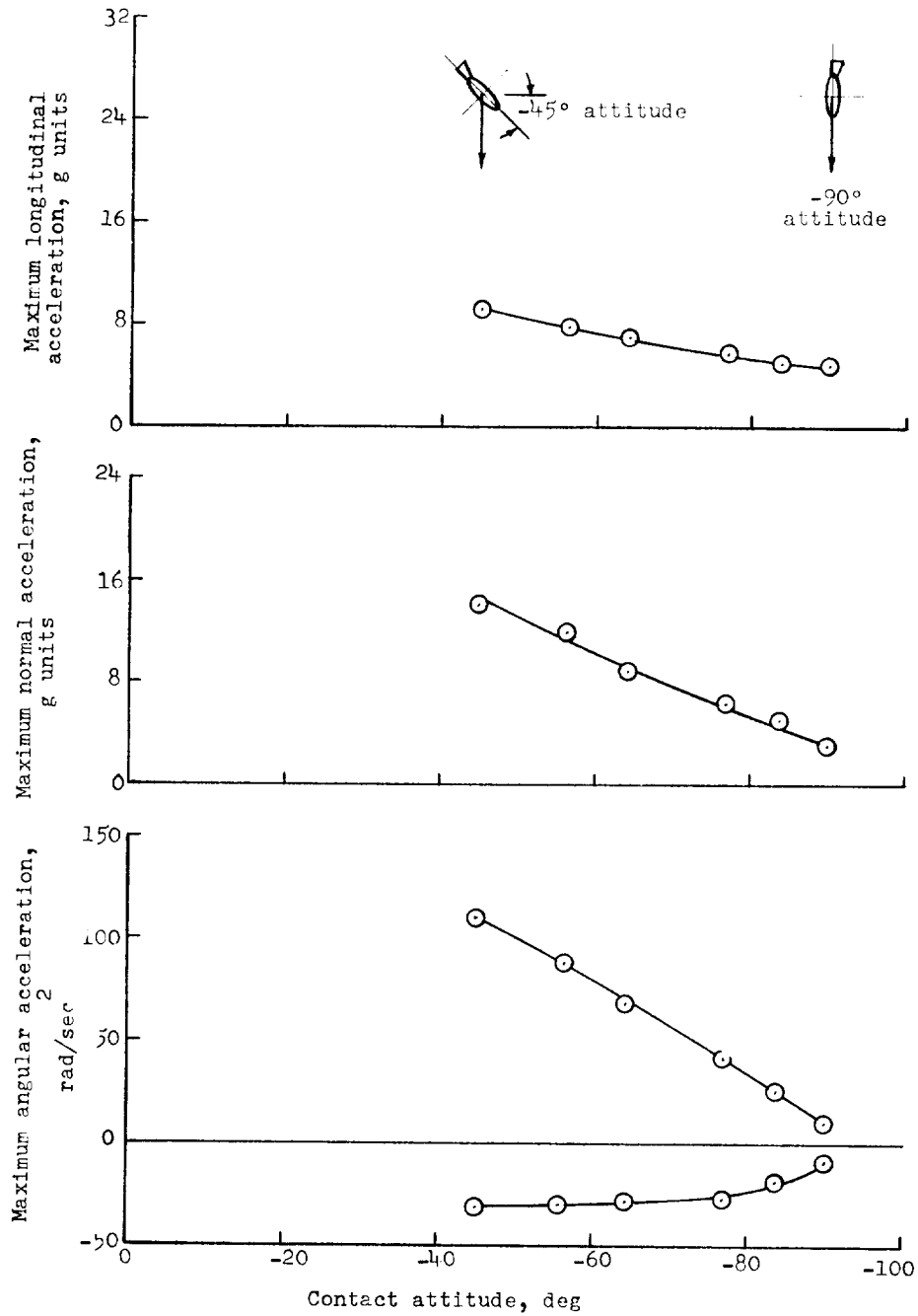
Figure 19.- Maximum accelerations obtained during vertical landings in water at various leading-edge contact attitudes. Flight-path angle, 90°; gross weight, 5,100 pounds; vertical velocity, 70 feet per second.